STRAIN VARIATION IN MORTAR JOINTS

A.T. Vermeltfoort[1]

ABSTRACT

Thirty three masonry discs, 25 mm thick, cut from couplets, were tested in compression. Specimens in the shape of discs were needed to allow for deformation measurements with ESPI, a laser speckle method. Three load cells made it possible to calculate the load eccentricity. General purpose (GP) mortars (15 mm) medium mortars (MM) (8 mm) and thin layer (TL) mortars (4 mm) were applied in combination with five brick types.
In average, the strength of the discs was 1.5 times the strength of prisms made of the same materials. However, Young's modulus was the same for both specimen types. Comparison of ESPI and LVDT results, in combination with measured reactions showed bending in the specimens. Variation of load eccentricity was found when cracking of the discs occurred. The ESPI measurements showed large strain variations at the edges of the GP and MM mortar joints. For completely filled TL joints, strains were almost equally distributed over the full joint. In average, the E values of brick and mortar were of the same order of magnitude in each brick-mortar combination. Test results will be used for detailed numerical simulation of masonry behaviour.

Key words: ESPI, compressive behaviour, mortar, boundary conditions

[1]Assistant professor, Eindhoven University of Technology, Department of Structural Design, BKO, P.O. Box 513, Postvak 7, 5600 MB Eindhoven. The Netherlands.

INTRODUCTION

Analytical and numerical models for masonry mostly assume a uniform strain distribution across the joints. However, in practice material properties are not uniform across the joint for the following reasons:

1. The brick laying process. In the Netherlands, the mason puts the amount of mortar required for one brick on the wall. Then, a brick is squeezed into the fresh mortar, and some of the mortar is scraped against the head of the previous brick with the brick being placed, Figure 1. The surplus of mortar is scraped away and thrown back into the container. In the middle, the mortar is compressed and consequently, the edges and header joints are not always completely filled.
2. Rounding of the bed joint, caused during brick laying when a wall is slightly moved in its thickness direction, see e.g. [Haller] and [Sabha e.a.]. Shrinkage of mortar at the edges makes this effect worse.
3. Brick suction is another reason for variation of mortar properties [Groot]. For good brick laying, the moisture content of the bricks and the workability of the mortar are

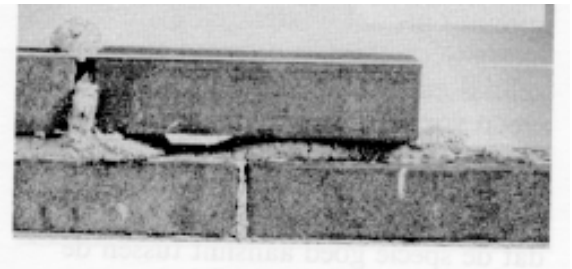

Figure 1. Example of a poorly filled joint (left)

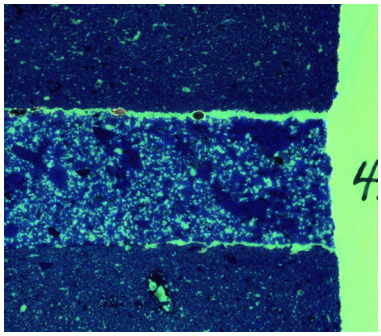

Figure 2 Photo of UV unit mortar interface

main parameters. As units absorb water from the mortar, large moisture variation in the transition between mortar and brick can occur [Groot] [Brocken e.a.].

4. Sanding of bricks sometimes caused poor bond because the sand worked as a kind of insulation. The grains of sand were well bonded by the mortar but they were only poorly connected to the brick. Some specimens, made with sanded HU bricks, (see Table 1) fell apart before testing. The layer of sand will deform differently from mortar and brick.
5. Experimental conditions, like load platen confinement, can cause an unequal strain distribution through the specimen too, as known from concrete e.g. [Vonk].

Figure 3. Examples of net bond area, 3 zones

Examples of these variations of mortar properties were found in bond wrench and tensile tests. In the example of Figure 3 only the middle surface of the bed joint had been bonded, Two other zones can be recognized: an outer zone with no bond at all, and a middle zone that shrank loose.
Figure 2 shows a photo taken under UV light of a section perpendicular to the bed joint.

The specimen was impregnated with epoxy resin and a material that reacted to UV light. Horizontal cracks, even before testing, are clearly visible.
As material properties are not uniform across the joint this will have its effects on brick mortar interaction and strain distribution. Therefore, the main goals of the project were

a) to establish the deformation behaviour in compression of mortar and bricks separately in combination with the effects of joint imperfections due to the 'brick laying process' and shrinkage,
b) to establish effects of joint thickness on deformation behaviour,
c) to obtain a data base of masonry behaviour in detail,
d) to establish the fracture process of small discs in comparison with that of prisms

The results will be used in subsequent numerical research where joint behaviour will be modeled in detail. ESPI results can be easily compared with strain distributions found with numerical simulations.

TEST SET UP

Thirty-three masonry discs, 25 mm thick, cut from couplets, were tested in compression. Discs were needed to allow for deformation measurements with ESPI, a laser speckle method (see par. 0). One of the conditions to obtain good results with ESPI is that the deformation at the specimens outside is representative for its behaviour. When, for instance, shrinkage cracks perpendicular to the observed surface are present, the surface will not come under full stress and deformations will not be representative for the behaviour of the specimen. By cutting a disc, its cutted surface will come under full compression and the effect of cracks and inhomogeneous joints still can be observed, Figure 4.

Figure 4. RW couplet and RW disc after testing

Materials

General purpose (GP) mortars (15 mm) medium mortars (MM) (8 mm) en thin layer (TL) mortars (4 mm) were used in combination with five brick types to build couplets and prisms [Pluijm]. Brick and mortar properties are presented in Table 1. All bricks used were 'waalformaat' i.e. $\pm 210 \times 100 \times 50$ mm^3.

Table 1 Brick and mortar properties

Brick		Type	f'br	f'brc	IRA	f"mo			E
						GP	MM	TL	
			MPa	MPa		MPa	MPa	MPa	MPa
Joosten	JW	Extrusion	141	70	3	18.2	22.3	32.8	29400
Heteren	HE	Extrusion	72	36	28	13.4	18.2	19.8	15100
Huissenswaard	HU	hand mould	37	19	35	13.0	15.9	9.4	8000
Rijswaard	RY	soft mud	26	13	44	9.6	9.4	10.1	54600
Hylkema	HY	light weight	17	8.4	47	9.9	10.3	9.2	3600

f'br = brick compressive strength NEN 2489 1976
f'brc = f'br with correction for h/t = 0.5 to h/t = 4 [Dutron]
f'mo = mortar compressive strength, NEN 3835
IRA = Initial Rate of absorption gr/dm^2/min
E = From tests or estimated on the basis of strength [Vermeltfoort] as E = 420 f'brc

Apparatus

The tests were carried out in a Schenck tensile machine in which a ‘compression-swing’ was mounted. The ‘compression swing’ has taken its name on the thick steel plate that was suspended with three steel bars from the upper traverse of the machine.
The specimen was positioned on this plate. Another thick plate on top of the specimen was mounted with thick steel rods down to the foundation of the machine. When the traverse of the machine was moved upwards, the bottom plate moved towards the top plate and the specimen was compressed. The bottom plate could move (‘swing’) freely in horizontal direction. Three load cells made it possible to calculate the eccentricity of the load.

Figure 5. Scheme of the ‘compression swing’

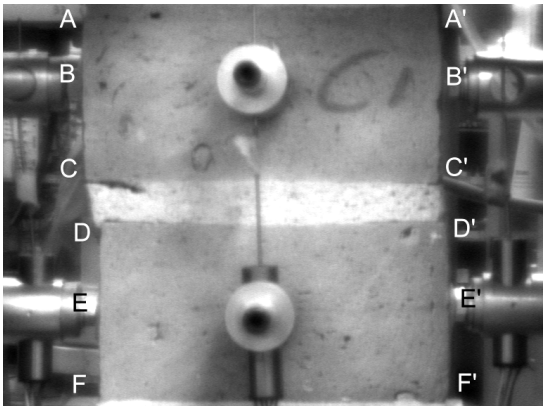

Figure 6 Specimen and instrumentation

Figure 7. Detail of ball hinge in Fig. 5

Measurements

Discs were capped with gypsum. The capping procedure did not allow for absolutely parallel surfaces which was compensated by the use of a ball hinge, see Figure 7.
Deformations of the specimen were measured with LVDT’s positioned in the middle of the surfaces of the specimen, Figure 6. Their gauge length was 60 mm with the joint in the middle. Deformation of the front surface of approximately 100×100 mm^2 was observed with ESPI. The ESPI system is explained in chapter 0. ESPI measurements

were taken at approximately one third of the estimated failure load.

RESULTS OF LVDT-MEASUREMENTS

Averaged compressive strengths of discs and E values are presented in Table 2. E values were established from LVDT measurements as the secant of the σ-ε diagram for values of σ between 10% and 80% of the strength.

Table 2 Averaged compressive strength and E values

	strength N/mm²			E value N/mm²		
	GP	MM	TL	GP	MM	TL
JW	43.1	46.5	59.3	14900	17300	22600
HE	29.8	31.2	48.9	6900	13400	14500
HU	11.3	16.5	17.2	1840	4120	4150
RY	12.1	16.3	12.6	3240	4300	4910
HY	11.8	10.4	7.6	4820	5120	4190

Compressive Strength

In average, disc strength was 1.5 times prism strength. Prisms were tested at TNO [Pluijm]. Possible causes for strength differences are: a) the number of joints in the specimen, b) the specimen size, c) the type of joints filling, d) experimental conditions

a) Only one joint was loaded in the discs. This is more favourable than the situation for a prism where load is transmitted from one joint via brick to another. Irregularities in the transition from brick to joint influence stress transfer in the next joint and brick. Prisms had relatively more brick than discs as well. Discs had only one joint; prisms had seven bed joints. Header joints in the prism made this situation even worse.

b) Specimen size effects were calculated according to [Dutron] and [Khalaf]. In Table 3 strength ratios are presented. Theoretically, differences in strength are not caused by slenderness differences.

c) Another difference is the way the joints were filled. Couplets were made by pushing the top brick vertically into the mortar. This procedure was a little different from the making of the prisms. For couplets the scraping of mortar to the header, Figure 1, was not necessary.

d) There was a difference in friction between load platens and specimen surface too. The discs were capped with gypsum, the prisms with masonry mortar.

Table 3 Strength ratio for discs according [Dutron] and [Khalaf]

Specimen size h×b×d	slenderness h/d	Dutron ratio	Khalaf ratio
disc 113×100×25 mm^3	4.5	0.744	0.394
prism 480×430×100 mm^3	4.8	0.716	0.391
Ratio disc / prism		1.04	1.01

Failure

Strong specimens failed much more suddenly then weak specimen. In particular JW specimens did not give any indication of the moment of failure. Fracture had an explosive character. Pieces were blown away for meters. The LVDT measurements showed a fast deformation increase in the final seconds of the test, Figure 8, left.
Completely different was the behaviour of HY specimens, where LVDT's gradually came loose from the specimens, e.g. Figure 8 right, where the right hand LVDT came loose from the surface. For softer masonry, failure also could be predicted during the test on the basis of the load-displacement behaviour recorded by the LVDT in the machine, by cracking of the specimen and some LVDT's which came loose from the specimen.

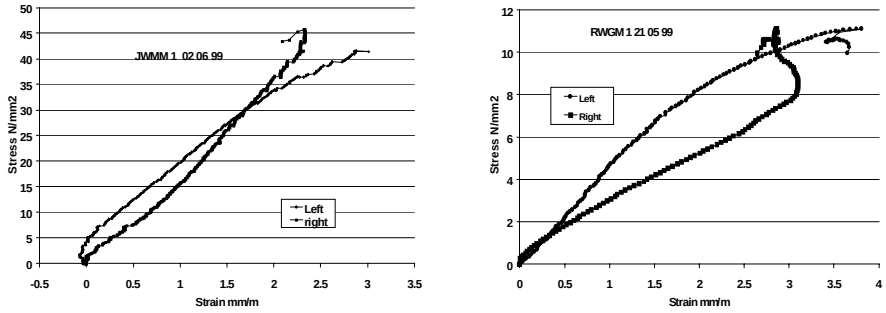

Figure 8. Stress-strain diagram for a RWGM disc and a JWMM disc

In specimens made from strong units and GP mortar, fracture lines were under an angle of 70° with the vertical direction and length wise with the disc specimen, as for concrete [Vonk]. Figure 9 shows an example with 70° fracture lines in the mortar and JO-bricks with a vertical fracture pattern.
In specimens made with softer bricks, e.g. RW, the crack ran right through the mortar into the brick and more diagonally through the disc. See also Figure 4.

Figure 9. JO and RW specimens after testing

Modulus of Elasticity

Prisms and discs, made from the same materials, roughly had the same E values. In average, Eprism was 0.97 times Edisc. The lower value of Eprism can be explained by the fact that a prism had five joints and a disc only one, resulting in a more irregular stress distribution for a prism as discussed in paragraph 0.
The linearity of the σ-ε diagrams was clear. The R^2 of the linear best-fit lines was more than 0.97 in all cases. Therefore, ESPI results were less sensitive for the stress level at which these measurements were taken. The E values established over the part of the σ-ε diagram where ESPI measurements were taken and those over the whole diagram differed in average only 2%.

Eccentricities

In all tests both LVDT's measured contraction, in many cases almost equal at both sides. In 15 tests the difference was smaller than 10% of the averaged value. Differences in LVDT results indicate eccentricities of the loading.
Load eccentricities also could be established from the reactions measured by the three load cells. The position of the resulting load in relation to the assumed center of gravity of the disc was calculated for each disc. As an example, the result of one RW disc is presented in Figure 10. Eccentricities were considerably smaller in the direction parallel to the surface observed with ESPI than in the perpendicular direction. For all tests the eccentricity in the direction parallel to the surface observed with ESPI was 1.02 mm in average. In thickness direction of the disc, the averaged eccentricity equaled 5.34 mm. In many cases the eccentricity varied considerably during one load step indicating that chips of a few mm thickness chipped off, Figure 10.
As a result of the fact that the load platens only had small rotations, the end surfaces of the specimen moved parallel to each other. The bottom plate, however, moved horizontally.

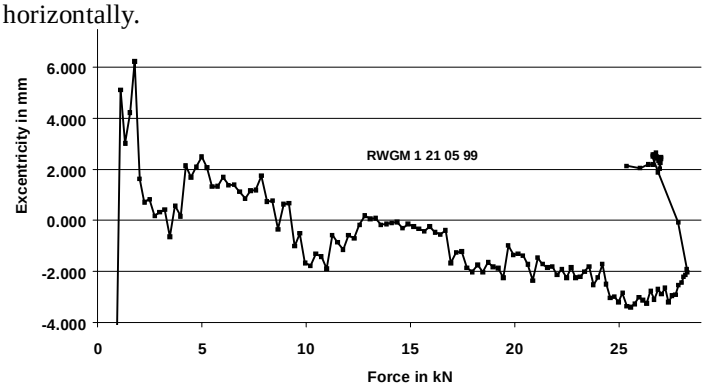

Figure 10. Eccentricity, after a begin-effect a slow decrease from +2 to –2 mm.
Bending moments as a result of the horizontal displacement of the swing

ESPI RESULTS

The ESPI System

ESPI is the abbreviation of **E**lectronic **S**peckle **P**attern **I**nterferometry [Jones e.a.]. The laser beam from the ESPI system is splitted in two and illuminates a surface from two sides. The reflected light is captured with a digital camera. The two lightbeams interfere and consequently speckle patterns develop. In each test, speckle patterns were taken at a load of approximately one third of the estimated failure load of the specimen and at a load approximately 2.5 kN higher ($\Delta\sigma = \pm$ 1 N/mm^2). By combining two speckle patterns, using the available software [Newport] fringe patterns were obtained. Fringe patterns contain information about the deformation of the surface due to an increase of the loading. From each fringe pattern the available software produced a file in which the displacements of approximately 50 by 70 points of the observed surface were stored. Basically, each of these files had one column for the X and one for the Y values of each point and a third column for the displacement of that point. Separate files were made for vertical and horizontal displacements. As an example, the vertical displacements of specimen RWGM 1 are plotted versus their X value in Figure 11.

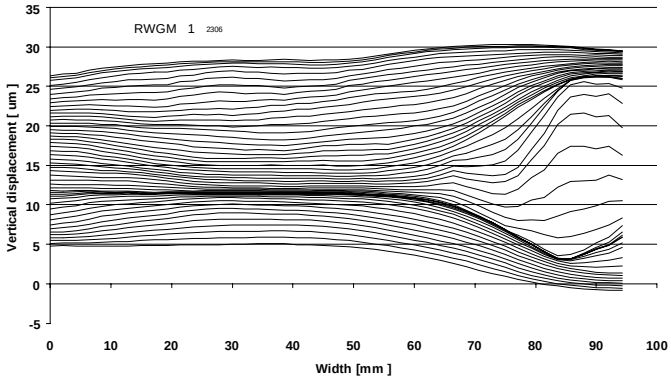

Figure 11. Vertical displacements versus horizontal position for RWGM 1

Vertical deformation and E values

From the displacements 'relative' strains were obtained as Ci = (vi-vj)/(yi-yj)/$\Delta\sigma$. These C values (C = Compliance) represent strains for a stress increase of 1 N/mm^2 obtained from the difference of the displacements of the points i and j (vi-vj) divided by their distance (yi – yj). Figure 12 shows two examples. For each specimen, C values were calculated over the top brick (yi=0 mm; yj = 48 mm) over the joint (yi = 48 mm; yj = 68 mm) over the bottom brick (yi=68 mm; yj = 105 mm) and over the same length as the LVDT measurements (yi=25 mm; yj=85 mm). These positions correspond with the height of lines AA' through FF' in Figure 6.
In some additional tests a LVDT was positioned in the middle of the surface observed with ESPI and consequently C values could not be established in that area, Figure 12 right. These measurements showed that ESPI and LVDT results were much the same.

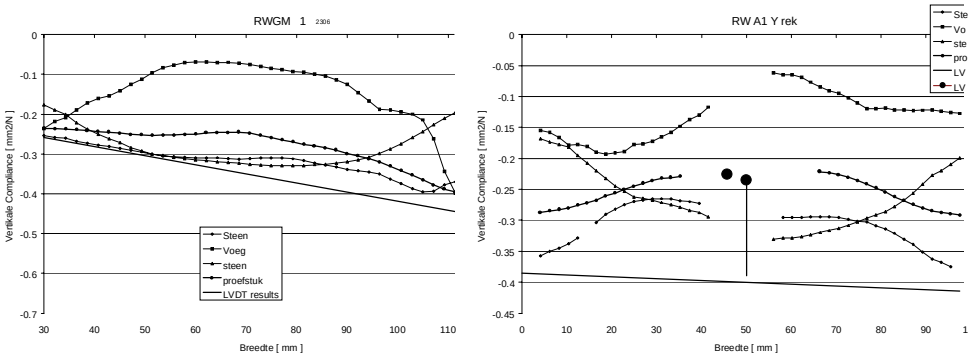

Figure 12 C value distribution over the width for a RWGM specimen, left, and RWA1.

C-values were averaged over the width of the specimen and where necessary E was calculated (E = 1/C). Than, the ratios Rmortar = Cspecimen / Cmortar and Rbrick = Cspecimen / Cbrick were calculated. The results are presented in Table 4, together with the E value from the LVDT results. As the stresses at the observed surface were not always equal to the applied stress (F/A) due to eccentricities in the load, ratios are given.
In general, Ebrick was 1.14 times Emortar.
When HE values were omitted Ebrick was 1.09 Ejoint.
The sum of Rmortar and Rbrick is not necessarily equal to one while the mortar part and the brick part are not of equal size. In addition, Rbrick was established over the full brick height (lines AA–BB or CC–DD in Figure 6) while Especimen was established over joint and brick, lines EE–FF.
Comparison of Rmortar with Rbrick shows that in most cases differences are in the order of magnitude of 0.10. Largest differences were found for HE and HY specimens. However, as all mortars were unique, a general tendency for the effect of joint thickness could not be established.
Differences were smallest for weaker brick types with MM and TL joints. JW en HE bricks had a relative weak mortar compared to brick stiffness. Mortar stiffness of TL mortars combined with relatively weak bricks like RY en HY is high.

Table 4 ESPI results (averaged). E values of specimen and ratios for bricks and mortar

specimen	R_{mortar}	R_{brick}	E value	specimen	R_{mortar}	R_{brick}	E value
JWGM	0.97	1.11	14900	RYGM	1.18	1.00	3240
JWMM	1.06	1.12	17300	RYMM	0.96	1.04	4300
JWTL	0.93	1.09	22600	RYTL	1.38	0.93	4920
HEGM	0.61	1.72	6900	HYGM	1.41	0.97	4820
HEGM	0.72	1.38	13400	HYMM	1.17	1.07	5120
HETL	0.95	1.21	14500	HYTL	1.44	1.31	4190
HUGM	0.81	1.19	1840	E values for brick are given in Table 1			
HUMM	1.33	1.02	4120				
HUTL	1.12	0.87	4150				

Joint behaviour

In the previous paragraph, the averaged C values were used to establish the R values presented in Table 4 in order to generally compare brick, mortar and masonry stiffness. This comparison only holds partly because the strain and neither stress distribution over the joint is not equal, e.g. due to shrinkage-cracking. Consequently, the larger strains at the edges increase the average but do not give insight in the mortar stiffness.
The graphs in Figure 13 were made as follows. First, the average strain was calculated for the area between 20 mm from the edges of the bricks (lines CC' + DD' in Figure 6). Than, the ratio between measured strain and averaged strain is plotted versus width. Consequently, the values in the middle, for x between 20 and 80 mm, vary around the value 1. At the edges, the ratio is much higher. The ratio is independent from the applied stress. The ratio is depended form the dimension of the middle zone. This dimension was based on experiences with shrinkage depth and visual observation of ESPI graphs. The chosen size of the middle zone shows effects most clearly.
For specimens with TL mortar, the line oscillates around the value one over the full width of the specimen. Specimens with GM and TL mortar have much larger values at the edges indicating larger deformations.

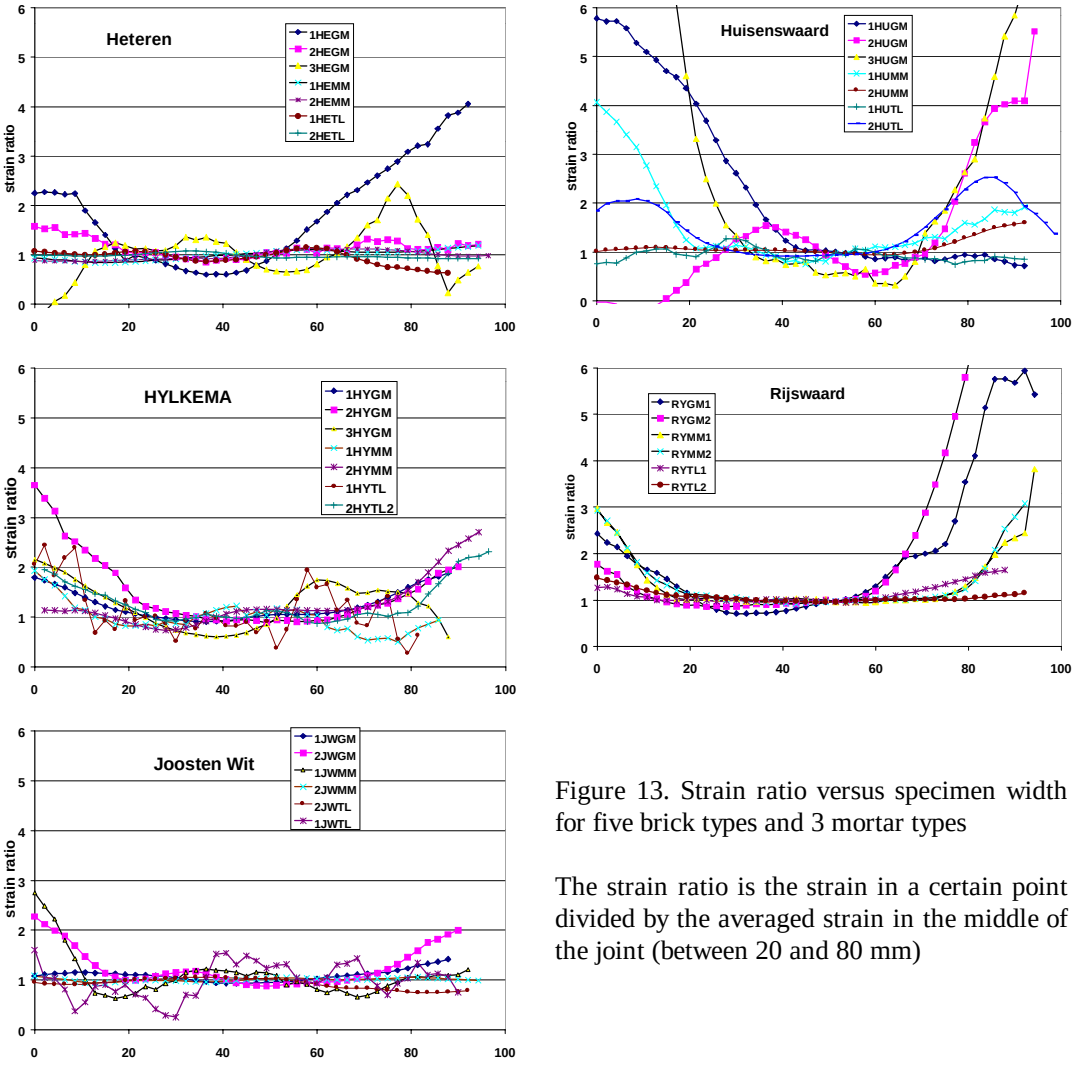

Figure 13. Strain ratio versus specimen width for five brick types and 3 mortar types

The strain ratio is the strain in a certain point divided by the averaged strain in the middle of the joint (between 20 and 80 mm)

Comparison of the graphs in Figure 13 shows clearly the tendency that strains at the outside are much larger than the averaged strain in the middle part of the specimen. For softer bricks like HY, strains deviate much more than for stiffer bricks like JW.
Brick behaviour is complementary to mortar behaviour. Large mortar deformation in combination with small brick deformation (or the other way around) results in the more or less uniform deformation of the specimen as a whole as measured with LVDT's. However, the smaller strains in the bricks at the edges close to the joint are masked by the more averaged strains in the center of the bricks.

Lateral deformation

Similar with vertical deformations the horizontal deformations were established too.

Figure 14 shows an overview of the horizontal strains for the RW specimens, calculated from: (vi-vj)/(xi-xj) where (xi-xj) equals the width of the specimen. The smaller deformations (and stresses) influence the strain distribution at the edges of the bricks, and of course by the difference in material properties. The position of the joints is clearly visible. Not all tests gave reliable results because horizontal deformations were too small. The structure of the observed surface played a part too.

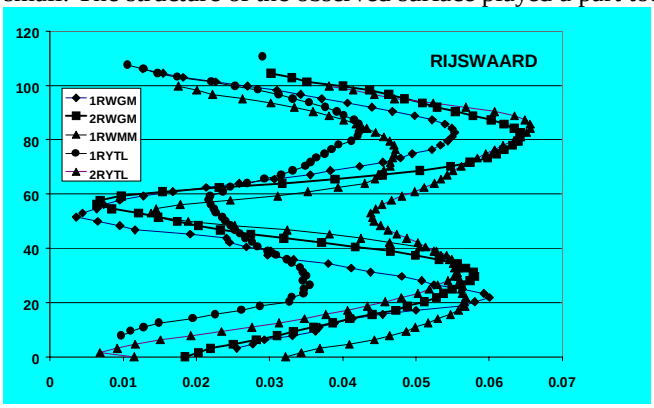

Figure 14. Example of horizontal strain distribution over height for 5 RW specimen

DISCUSSION / CONCLUSIONS

- Specimens in the shape of discs were needed to allow for deformation measurements with ESPI, a laser speckle method.
- In average, disc strength was 1.5 times the strength of prisms made with the same materials. Main cause is the fact that a disc only has one joint, compared to the seven joints in the prism. However, Young's modulus was the same for both specimen types. In general, discs behaved more brittle than prisms, strong discs even 'exploded'.
- Stress strain diagrams of discs obtained with LVDT's were almost linear.
- The three load cells in the compression swing that was used made it possible to calculate the eccentricity of the load. Compared with ESPI and LVDT results, the effects of bending in the specimen were estimated. The largest effects on strain distribution were found in thickness direction. Variations of load eccentricity in the widest direction were found when pieces of brick chipped of from the discs.
- Load platens moved parallel to each other. Horizontal movements of the bottom plate caused bending moments.
- For GP and MM mortar joints the ESPI measurements showed large strain variations at the edges of the observed surface. For completely filled TL joints, strains were almost equally distributed over the full joint. In average, in each brick-mortar combination the E values of brick and mortar were of the same order of magnitude. In average, values found with ESPI resulted in Ebrick = 1.14 Ejoint
- Lateral deformations show effects on the deformation of the joint. The order of magnitude of the lateral strain at a vertical load of 1 N/mm^2 is equal per brick type.

As lateral deformations were smaller than vertical they were more difficult to establish.

- Mortar compressive strength is much smaller than brick strength (Table 1), however E values are almost equal. As the mortar hardened in a steel mould its properties were different from the mortar that hardened between bricks [Vermeltfoort 98].
- Test results will be used for detailed numerical simulation of masonry behaviour. Next step in the project is the study of the effects of larger eccentricities (bending) on the joint.

ACKNOWLEDGEMENTS

The financial support of 'De stichting Stapelbouw' (the Dutch Masonry Foundation) is gratefully acknowledged. Participating in the foundation are the clay brick, calcium silicate and concrete units industries and mortar manufacturers.

REFERENCES

Brocken, H.J.P., Van der Pers, N.M. and Larbi, J.A., 2000, Composition of lime-cement and air-entrained cement mortar as a function of distance to the brick-mortar interface: consequences for masonry, Mat. and Stru. Vol. 33, pp 634-646

Dutron, 1980, in: Ontwerp en berekening van Metselwerk. Belgisch Instituut voor normalisatie. Belgium Building Code. NBN 24-301.

Groot, C., 1993, Effects of water on mortar-brick bond, PhD Thesis, Delft

Haller P., 1958, (Dutch translation 1967), "Die technische Eigenschaften von Backstein", Schweizerische Bauzeitung.

Jones, R. and Wykes, C., 1989, " Holographic and Speckle Interferometry" ISBN 0 521 23268 6, 2nd edition, Cambridge University Press, Cambridge.

Khalaf, F.M. and A.W. Hendry, 1994, Masonry unit shape factor from test Results, Proc. 3th Int. Mas. Conf., Stoke on Trent, pp. 136-140.

Newport, 'Brochure of the ESPI SD-30 system', Newport Instruments AG Giessenstrasse 15, CH-Schlieren, Switserland.

van der Pluijm R., 2000, TNO Rapport

Sabha A. and Schöne I., 1994, 'Untersuchungen zum Tragverhalten von Mauerwerk aus Elbesandstein' Bautechnik (Ernst & Sohn Verlag) Nr 71, pp 161-166.

Vermeltfoort, A.T., 1997, Properties of Some clay bricks under varying loading conditions, Mas. Int. Vol. 10, No. 3, pp 85-91.

Vermeltfoort, A.T., 1998, Mechanical compressive properties of small sized mortar cylinders, 8th Can. Mas. Symp., Jasper, pp 336-347.

Vonk, R.A., 1992, Softening of concrete loaded in compression, PhD Thesis. Eindhoven University.